1180 *Russian Chemical Bulletin, International Edition, Vol. 58, No. 6, pp. 1180—1191, June, 2009*

Photochemical transformations of chalcone-podands into cyclobutane-containing benzocrown ethers*

I. G. Ovchinnikova, O. V. Fedorova, E. G. Matochkina, M. I. Kodess, P. A. Slepukhin, and G. L. Rusinov★

I. Ya. Postovsky Institute of Organic Chemistry, Ural Branch of the Russian Academy of Sciences,
22/20 ul. S. Kovalevskoi, 620041 Ekaterinburg, Russian Federation.
Fax: +7 (343) 374 1189. E-mail: iov@ios.uran.ru

A method for the synthesis of cyclobutane-containing benzocrown ethers by the template photocycloaddition of the corresponding chalcone-podands in solutions was developed. It was shown by X-ray diffraction analysis, ^{1}H and ^{13}C NMR, and UV spectroscopy that the intramolecular [2π+2π] photocycloaddition (PCA) is stereoselective with the predominant formation of structures of the β- and γ-truxinic type. The PCA rate was shown to depend on the size of the oxyethylene spacer and stereoorientation of the chalcone fragments in the podands. The selectivity of the PCA process can be controlled by a change in the concentration of the template (alkaline metal ions) and variation of the wavelength range of irradiation.

Key words: chalcones, podands, crown ethers, [2+2] cycloaddition, cyclobutanes, photochemistry.

The cinnamyl derivatives (chalcones) prone to photoinduced [2π+2π] photocycloaddition (PCA) evoke increased interest due to a possibility of using them as ligands with the photocontrolled properties.[1—3] However, the choice of this type of compounds as molecular switchers requires high regio- and stereoselectivity of PCA processes.[4] The regioselectivity of pericyclic reactions depends on the pre-organization of the reacting ethylene groups. Two types of cycloaddition are possible: "head-to-head" or "head-to-tail." [4,5] It is *E*-isomers that are usually involved in the PCA reaction. At the same time, conformational transitions of chalcones can affect, to a considerable extent, the reactivity of the CH=CH bonds and stereoisomerism of the PCA products.[6] As a rule, the photoinduced dimerization reactions of cinnamic acid derivatives in solutions occur with low stereo- and regioselectivity and afford a mixture of cyclobutane-containing stereoisomers including those with the α-, ε-truxillic and β-, γ-truxinic structures.[4,5] However, on going to macromolecules (crown ethers, podands) capable of pre-organization, the regio- and stereoselectivity of the PCA processes were considerably enhanced in some cases.[1,2] For example, the principle of valence pre-organization of ethylene groups in chalcone-containing cyclophanes was used to obtain cyclophanes with cyclobutane fragments.[7—11] A noticeable selectivity of the intramolecular photocycloaddition process in noncyclic analogs of dibenzocrown ethers (podands) with the terminal vinyl groups in the *para*-position to the polyether chain was provided by the stacking interaction of the aromatic substituents.[12—14] However, attempts to enhance the selectivity of the PCA process, including the use of metal cations as templates, by irradiation of solutions of the podands containing cinnamic acid residues in the 1,ω-positions were unsuccessful.[15,16]

We have earlier studied[17] the influence of the pre-organization of the chalcone-podand molecules with the propenone group in the *ortho*-position of the bridging aryl

Scheme 1

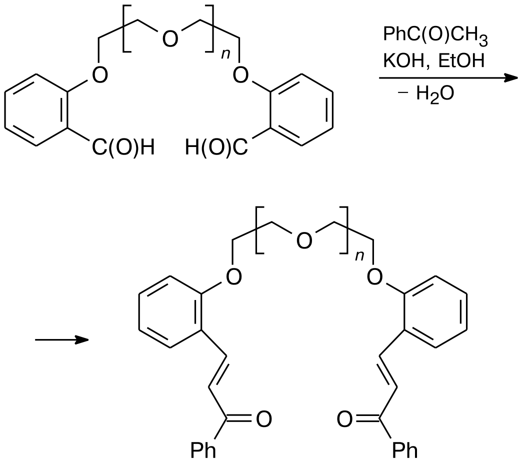

1a—c

n = 0 (**a**), 1 (**b**), 2 (**c**).

---

* Dedicated to Academician O. N. Chupakhin on the occasion of his 75th birthday.

Published in Russian in *Izvestiya Akademii Nauk. Seriya Khimicheskaya,* No. 6, pp. 1150—1160, June, 2009.

substituent to the oxyethylene fragment in crystals on their ability to undergo topochemical intermolecular PCA reactions. Based on the X-ray diffraction data, we predicted the highest probability of the photochemical [2+2] cycloaddition in the solid phase for the podands with the phenyl substituents and oxyethylene fragment containing two or three oxygen atoms (**1a**,**b**) (Scheme 1). In the present work, in order to develop methods for the synthesis of cyclobutane-containing crown ethers, we studied the tendency of chalcone-podands **1a**—**c** to undergo PCA transformations in solutions and the influence of such factors as the template effect and pre-organization of ligands on the regioselectivity of intramolecular [2π+2π] photocycloaddition.

Results and Discussion

Stereoorientation of the chalcone groups in podand molecules **1a**—**c** has a decisive significance in photocycloaddition processes. Judging from the vicinal spin-spin coupling constants (SSCC) of the olefinic protons in the ^{1}H NMR spectra, the products of the Claisen—Schmidt aldol condensation (see Scheme 1) are predominantly formed as *E*-isomers (Table 1). The chemical shifts of these protons are very close, and their identification from usual ^{1}H NMR spectra is difficult. The unambiguous assignment of ^{1}H and ^{13}C signals was performed using 2D ^{1}H—^{13}C HSQC and HMBC experiments. In the ^{13}C NMR spectra, the signals for the olefinic carbon atoms differ significantly in the chemical shifts: $\delta_{C_\alpha} \approx 122$ and $\delta_{C_\beta} \approx 139$, which makes it possible to identify the corresponding protons by the 2D HSQC data (see Table 1). This assignment is also confirmed by the results of 2D HMBC experiments in which the cross-peaks between the nuclei pairs H(6)—C(β) and H(β)—C(2) are observed. It is noteworthy that the positions of the signals for the olefinic protons in the ^{1}H NMR spectra change with the elongation of the oxyethylene fragment in compound **1**: at $n = 0$ (**1a**) the signal of the H_α proton appears in a lower field and the difference in the chemical shifts $\Delta_{\alpha\beta}$ is 0.16, whereas at $n = 1, 2$ (**1b**,**c**), it is the H_β protons that undergo a downfield shift and the $\Delta_{\alpha\beta}$ difference decreases substantially.

According to the X-ray diffraction data,[17] the propenone fragment of chalcone-podand molecules **1a**,**b** exists in the *trans-s-cis* conformation and is stabilized in crystals as structure **A** (Fig. 1). The *s-cis* conformation is confirmed by the results of 2D ^{1}H—^{1}H NOESY experiments for solutions of compound **1** in DMSO-d$_6$. However, the analysis of the intensity of the cross peaks suggests that the elongation of the oxyethylene fragment facilitates the conformational transition due to the rotation about the C(1)—C$_\beta$ bond from structure **A** characteristic of compound **1a** to structure **B**, which is more preferential for compounds **1b**,**c**. The decrease in the energy barrier to rotation is due, probably, to the elongation of this bond to 1.460(2) Å for compounds **1b**,**c** compared to 1.438(2) Å for compound **1a** (X-ray diffraction data).[17] In our opinion, this transition explains the above changes in chemical shifts of the protons of the CH=CH fragment in compounds **1a**—**c**.

Table 1. ^{1}H and ^{13}C NMR spectral parameters of the CH=CH fragment in compounds **1a**—**c**

Compound	δ					$^3J_{H_\alpha,H_\beta}$/Hz
	H_α	H_β	$\Delta_{\alpha\beta}$	C_α	C_β	
1a	8.02	7.86	0.16	122.65	139.81	15.9
1b	7.96	8.02	−0.06	122.33	139.15	15.8
1c	7.97	7.99	−0.02	122.27	139.24	15.8

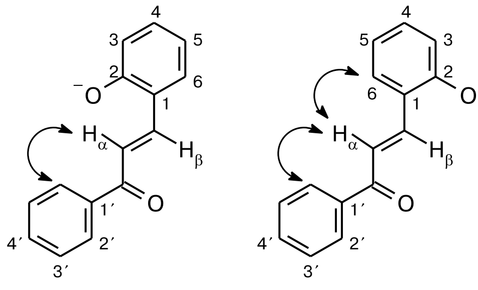

A (**1a**) **B** (**1b**,**c**)

Fig. 1. Stereoorientation of the enone in compounds **1a**—**c** (arrows show the main correlations observed in the 2D NOESY experiment).

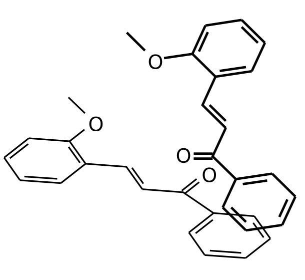

A

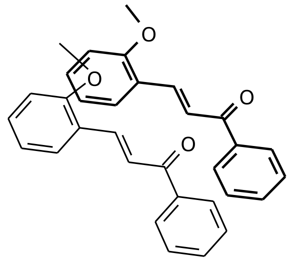

B

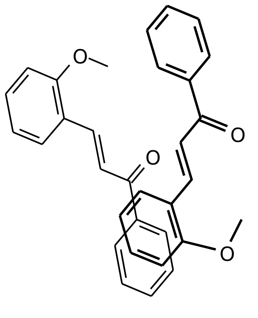

C

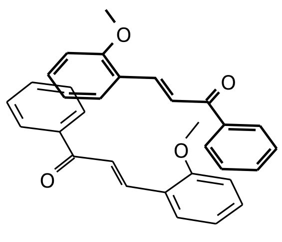

D

As a rule, the mechanism of photoinduced [2π+2π] cycloaddition for olefins (chalcones) is associated with two routes of photochemical activation of the reactant: through the singlet state or through triplet excited state due to intersystem crossing.[18] In the former case, the concerted (through the formation of an excimer) PCA process occurs allowed by orbital symmetry. Taking into account that the *trans-s-cis* conformation of the chalcone fragment of compounds **1a—c** is most stable, the following variants of intramolecular [π+π] complex formation are possible: *anti*-, *syn*-"head-to-head" or *anti*-, *syn*-"head-to-tail" (**A**, **B**, **C**, and **D**, respectively). In the second case, the reaction predominantly proceeds according to the radical mechanism to form the intermediate 1,4-biradical.[19]

The irradiation of solutions of chalcone-podands **1a—c** in DMF or MeCN with both the non-filtered light from the incandescent lamp (150 W) and the filtered light from the mercury lamp (500 W) in the short-wavelength ranges with λ_{max} = 366 and 405 nm resulted in the formation of mixtures of the starting compounds and photolysis products that were difficult to separate. According to the ^{1}H NMR spectral data, the *E*—*Z*-isomerization processes occurred predominantly (35—40%) in all the three cases. The presence of *Z*-isomers was confirmed by the appearance of the signals for the protons of the CH=CH fragment of the enone at δ 7.27 and 6.66 as doublets with an SSCC of 12.7 Hz. In addition to the signals for the protons of the starting podands and *Z*-isomers, the spectra contained characteristic signals of the AA´BB´ spin system, which are attributed to the stereoisomeric cyclobutane products. In the case of compound **1a**, the major cyclobutane derivative was compound *rtct*-**2a**, whereas isomeric cyclobutanes *rctt*-**3b,c** and *rttc*-**4b,c** were formed in the case of compound **1b,c** (Scheme 2).

Along with compound **2a**, the ^{1}H NMR spectra of the reaction mixture exhibit trace amounts of two other isomeric cyclobutane-containing crown ethers with the signals for the protons of the four-membered cycles at δ 5.68 and 3.82, as well as at δ 5.06 and 4.53. These signals may belong to *rtcc*-**3a** and *rctt*-**4a**, respectively (Scheme 2, Table 2).

The content of the cyclobutane isomers in the mixture varied from 7 to 18%. On going from the visible light-irradiation of chalcone-podands **1b,c** to the ultraviolet region, the fraction of cyclobutanes *rtcc*-**3b,c** increased noticeably (from 2 to 12%). The decrease in the amount of chalcones **1b,c** due to the photochemical reactions is observed in the electronic absorption spectra as well. The decrease in the intensity of two long-wavelength absorption maxima at 344 and 298 nm that characterize the conjugation system of the chalcone fragment after the irradiation of the solutions for 2—3 weeks was accompanied by the simultaneous hypsochromic shift of the maximum at 298 nm by 16 nm (Fig. 2). The decrease in

Scheme 2

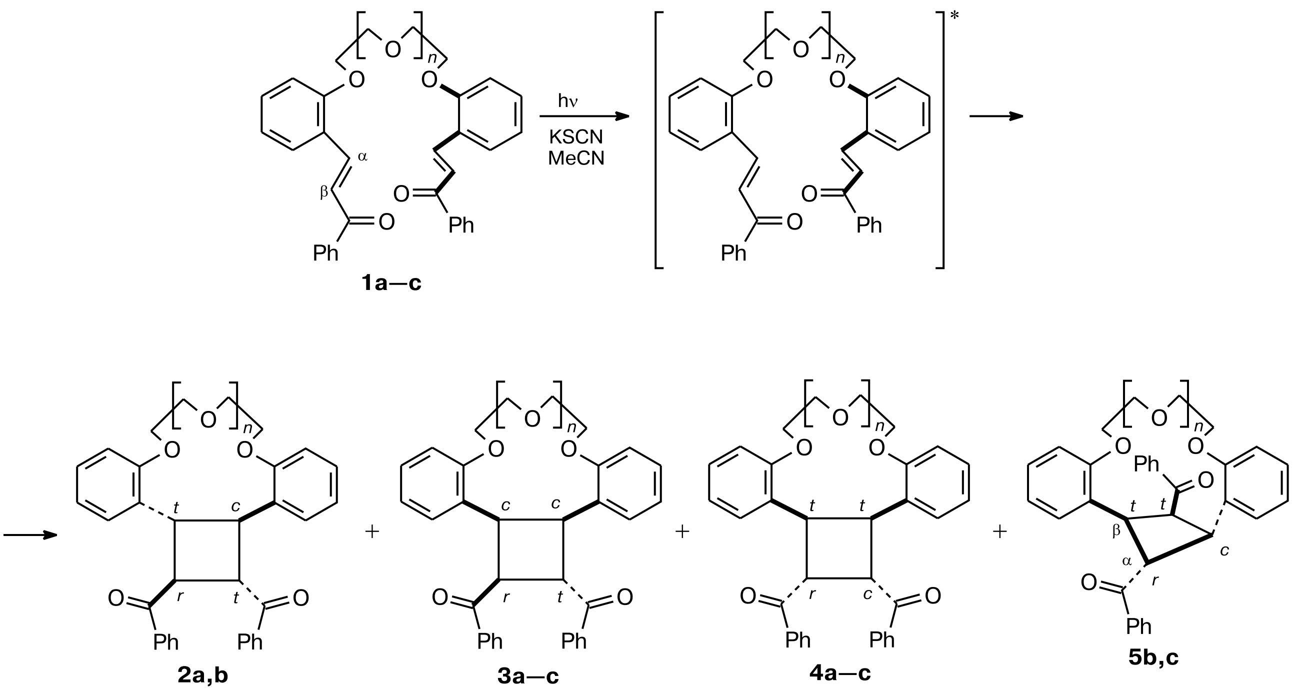

n = 0 (**a**), 1 (**b**), 2 (**c**).

Table 2. Ratio of the PCA products after the irradiation with the filtered light from the mercury lamp (500 W) of acetonitrile solutions of chalcone-podands **1a—c**

Ratio of reactants	T^a/nm	Ratio of stereoisomers (%)			
1a : KSCN		**2a**	**3a**	**4a**	**5a**
1 : 1	258—400	94	5	—	—
	364—456	90	4	5	—
1b : KSCN		**2b**	**3b**	**4b**	**5b**
1 : 1	258—400	15	73	—	12
	364—456	53	34	6	7
1 : 3	258—400	36	50	—	7
	364—456	70	16	9	5
1 : 6	258—400	40	14	40	6
	364—456	44	9	44	3
1c : KSCN		**2c**	**3c**	**4c**	**5c**
1 : 1	258—400	—	71	13	16
	364—456	—	21	70	9
1 : 3	258—400	—	50	43	7
	364—456	—	10	82	8

[a] *T* is transmission.

the degree of conjugation of the chromophores is related, correspondingly, to both the formation of the PCA products and transformation of the *E*-isomer into the *Z*-isomer.[20,21]

On the basis of specific features of the structures[17] of the starting compounds **1a—c**, it can be assumed that the simultaneous influence of the *gauche* effect[22] from the oxyethylene fragment providing the approach of the terminal groups of the ligands (4.2—8 Å, X-ray diffraction data)[17] and the kinetic template effect[22] from the K^+ (Li^+, Cs^+) ions can enhance the regio- and stereoselectivity of the intramolecular PCA process due to the shortening of this distance.

In fact, the electronic absorption spectra of irradiated solutions of compounds **1a—c** in the presence of an equimolar amount of KSCN ($KClO_4$) exhibit rather fast exponential decrease in the absorbance. The complete disappearance of the long-wavelength absorption maxima at 298 and 343 nm indicated the occurrence of the PCA reactions (see Fig. 2). The dimerization processes of the chalcone-podands differ considerably in time. For compound **1b**, the reaction rate is fourfold higher than that for compounds **1a,c** (Fig. 2). First, it was natural to assume the influence of the correspondence of the size of the coordinating oxyethylene ligand cavity and the metal cation radius on the intramolecular dimerization rate. However, the use of the Li^+ cations (0.78 Å) for compound **1a** and Cs^+ cations (1.65 Å) for compound **1c** as templates only insignificantly shortened the reaction time (by 3—4 h). It is known that the podands are conformationally mobile compared to the crown ethers[23] and, hence, manifest a low complexation ability. Therefore, in our case, they form, most likely, complexes of the "roost" type, where the guest is arranged at the top of the binding (oxyethylene fragment) surface of the host.[24] That is why, other factors capable of influencing the rate and selectivity of the PCA process can be the polyether chain length and stereoorientation of the chalcone terminal groups of the podands. The problem on the degree of influence of

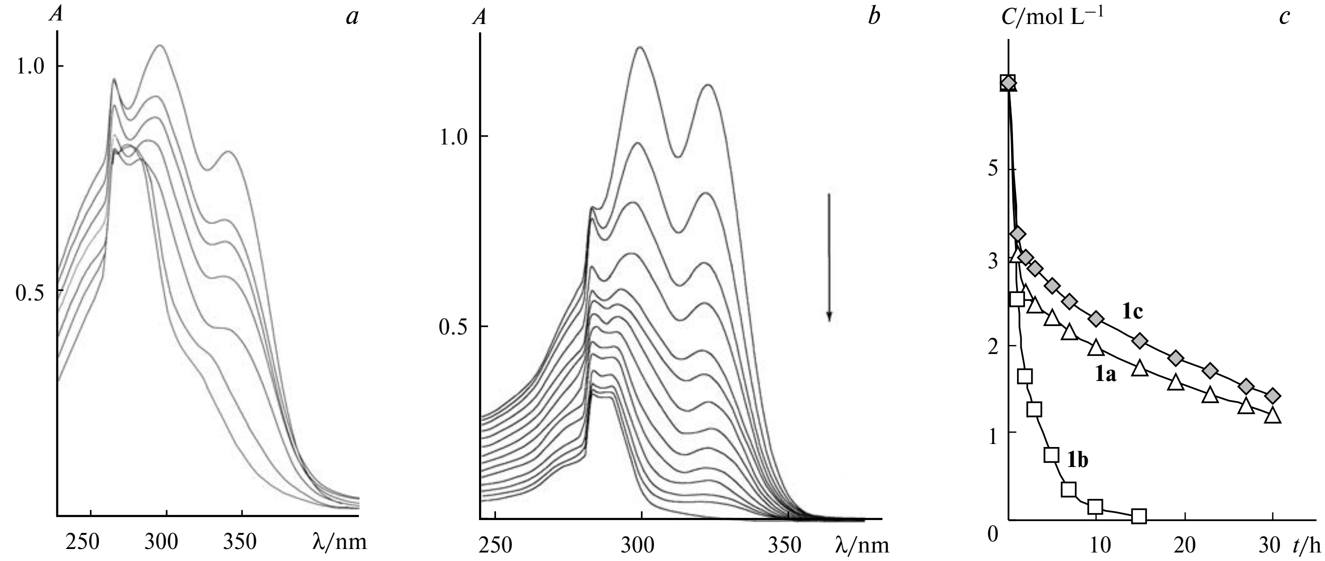

Fig. 2. Electronic absorption spectra of compounds **1a—c** ($c = 5 \cdot 10^{-5}$ mol L^{-1}) in DMF solutions during the irradiation with the light from the incandescent lamp (150 W) in the absence (*a*) and in the presence of the potassium cation (*b*); *c*, changes in the concentrations of compounds **1a—c** ($c_0 = 5 \cdot 10^{-5}$ mol L^{-1}) at 25 °C with time, *t*/h: 59 (**1a**), 15 (**1b**), and 67 (**1c**); $k_{app} = (1.3\pm0.2) \cdot 10^{-7}$ (**1a**), $(1.6\pm0.25) \cdot 10^{-6}$ (**1b**), and $(1.0\pm0.2) \cdot 10^{-7}$ (**1c**).

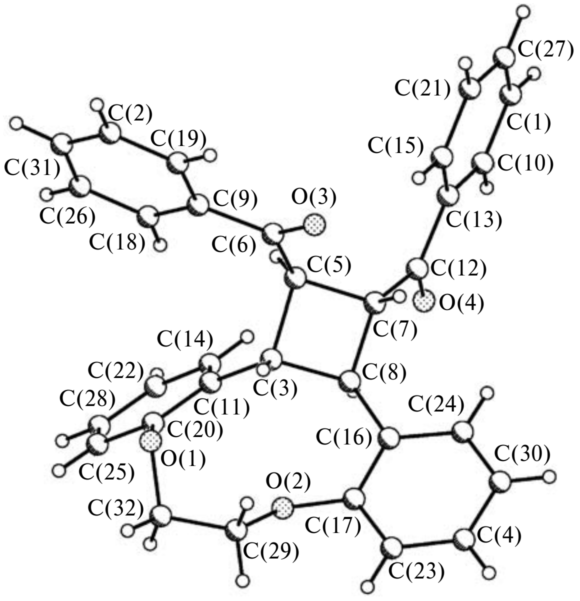

2a

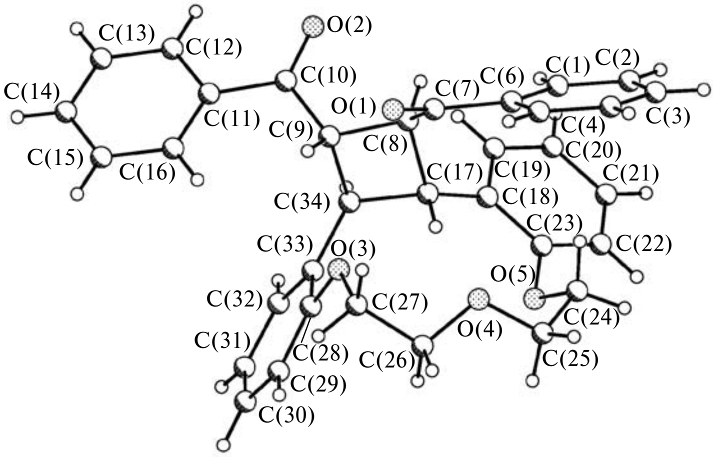

2b

Fig. 3. Geometry of molecules of crown ethers **2a** and **2b**.

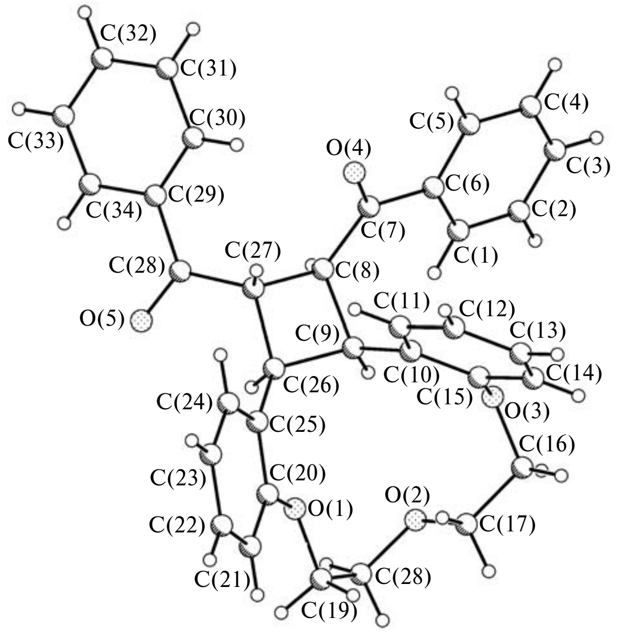

3b

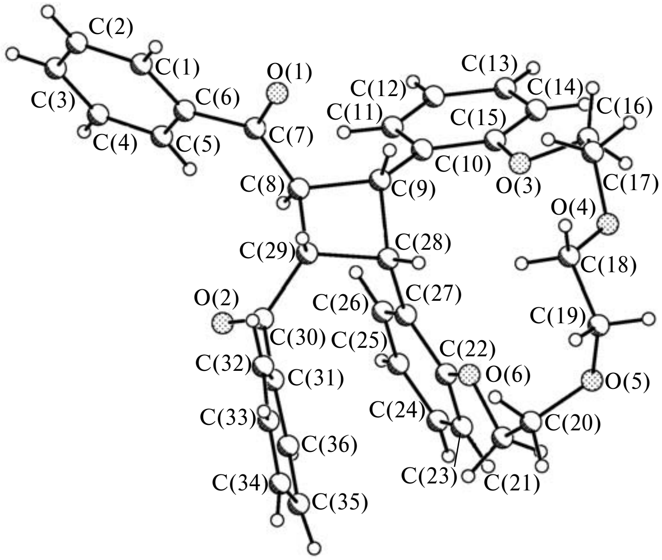

3c

Fig. 4. Geometry of molecules of crown ethers **3b** and **3c**.

the listed geometric parameters of the molecules was solved using X-ray diffraction analysis and NMR spectroscopy.

The equilibrium shift from the *E—Z*-isomerization processes toward the PCA reactions in the presence of equimolar amounts of KSCN in the studied solutions of podands **1a—c** was confirmed by the analysis of the ^{1}H NMR spectra of the reaction mixtures. However, some distinctions were revealed in the studied processes of photocycloaddition for compounds **1a** and **1b,c**. The irradiation of chalcone-podand **1a** with the filtered light in

Table 3. Parameters of the ^{1}H and ^{13}C NMR spectra of the cyclobutane fragment in compounds **2—4**

Compound	δ_H				δ_C			
	H_α	$H_{\alpha'}$	H_β	$H_{\beta'}$	C_α	$C_{\alpha'}$	C_β	$C_{\beta'}$
2a		4.75		4.01		45.44		41.85
2b		4.65		4.72		46.59		41.83
3b	4.85	5.52	5.35	4.75	48.22	41.64	38.64	37.88
3c	4.86	5.49	5.29	4.78	49.04	41.83	38.26	37.47
4b		5.00		4.63		47.24		37.74
4c		4.93		4.60		48.83		34.75

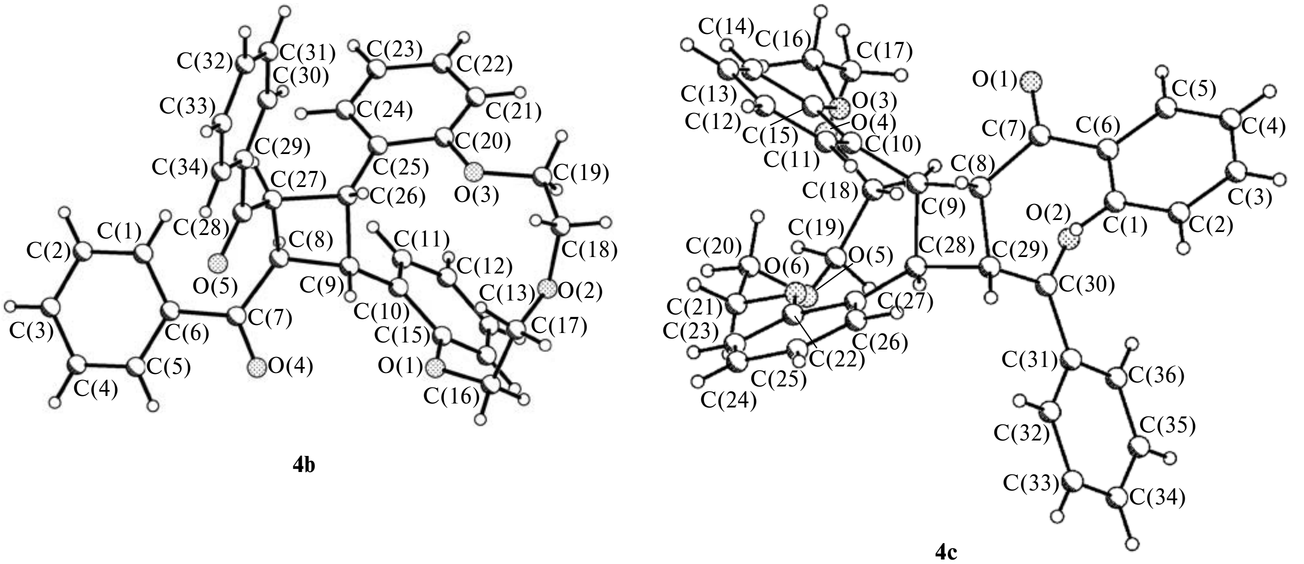

4b

4c

Fig. 5. Geometry of molecules of crown ethers **4b** and **4c**.

the wavelength range with λ_{max} = 366 and 405 nm in the solution resulted in the regiospecific intramolecular PCA with the predominant formation of crown ether **2a** containing the cyclobutane fragment of the γ-truxinic type with the characteristic spin system of signals for the AA´BB´ protons at δ 4.01—4.74 in the ^{1}H NMR spectra (see Scheme 2, Fig. 3, Tables 2, 3).

The pattern of intramolecular PCA processes became somewhat more complicated with the elongation of the oxyethylene fragment in the chalcone-podands on going from **1a** to **1b,c**. The formation of cyclobutanes *rtcc*-**3b,c** was predominantly observed upon the irradiation with the light with λ_{max} = 366 nm (Fig. 4), whereas upon the irradiation with the light with λ_{max} = 405 nm cyclobutanes *rtct*-**2b** (see Fig. 3) and *rctt*-**4c**, respectively, were predominantly formed (Fig. 5, see Scheme 2, Tables 2, 3).

The use of a considerable excess of the potassium salt in the studied solutions of compound **1b** led to the equiprobable formation of crown ethers *rtct*-**2b** and *rctt*-**4b** (Fig. 5, see Tables 2, 3), whereas for compound **1c** the further increase in the regio- and stereoselectivity of formation of photoadduct **4c** was observed.

It should be mentioned than the elongation of the oxyethylene fragment in the case of chalcone-podands **1b,c** allows another type of packing of the activated double bonds "head-to-tail" **C**, **D** to occur, which is allowed by the orbital symmetry. Indeed, insignificant amounts of 1,3-diphenacylcyclobutanes *rctt*-**5b,c** were found in the reaction mixtures (Table 2). The X-ray diffraction analysis of compound **5c** (Fig. 6) and the identical character of the ABCD spin system of the cyclobutane protons of compounds **5b,c** in the ^{1}H NMR spectra in the region δ 5.6—4.7 is evidently in favor of more energetically favorable variant of intramolecular packing **D**.

Thus, two routes of intramolecular cyclization, *viz.*, through both the singlet and triplet excited states, occur in the solution photolysis of chalcone-podands **1a—c**. The concerted PCA process allowed by the orbital symmetry is favored by the formation of photoadducts **2**, **4**, and **5** upon the irradiation of solutions of the chalcone-podands with the longer-wavelength light (λ_{max} = 405 nm). In this case, the kinetic template effect of potassium cations can provide an additional intramolecular approach of the activated CH=CH bonds of the chalcone fragments up to the formation of excimers. At the same time, the predominant formation of *rtcc*-isomers **3** due to the short-wavelength ultraviolet irradiation (λ_{max} = 366 nm) proceeds mainly through the 1,4-biradical mechanism. The presence of the benzoyl substituent at the CH=CH fragment of the chalcone favors, as is known, an increase

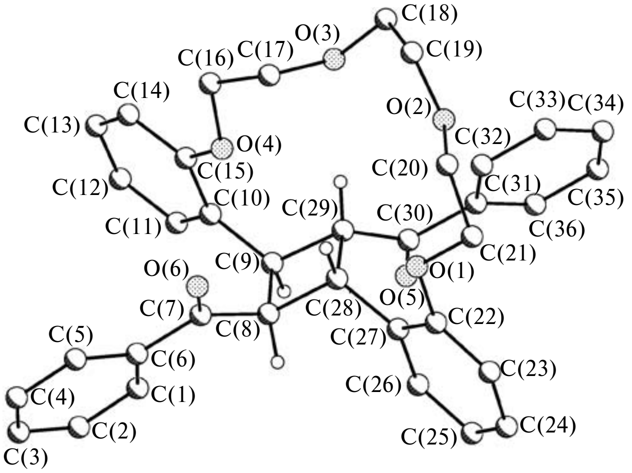

Fig. 6. Geometry of a molecule of crown ether **5c**.

in the constant of singlet-triplet conversion (sensitizing ability).[18] Two variants of formation of crown ethers **3** are possible. The first variant, which is more probable, in our opinion, is related to the primary formation of the σ-bond between the C_α carbon atoms of the adjacent chalcone groups. The triplet 1,4-biradical formed as a result of the intersystem crossing can undergo the conformational shift from the bulky bridging aryl substituents in the final stage of cyclization due to a longer lifetime than that of the singlet state. The second variant is associated with the *E—Z*-isomerization of one of the terminal groups of the chalcone-podand and, further, with the subsequent intramolecular photocycloaddition to form crown ether **3** (see Ref. 25). In the case of this route, the cyclization of compound **1a** would proceed only with the formation of stereoisomer **3a**, because the *E—Z*-isomerization is preferential for this chalcone-podand in the absence of the template. However, this is not observed.

Another factor affecting the rate and selectivity of the PCA reactions is the stereoorientation of the chalcone groups of the initial ligands. It follows from the X-ray diffraction analysis of photoadducts **2—5** (see Figs 3—6) that the chalcone-podands are involved in the intramolecular dimerization only in the *trans-s-cis* conformation. The reaction rate depends on the presence of more reactive structure **B** of the starting podand (see Fig. 1). In fact, as it was shown above, although compounds **1a** and **1b** have the same *s-cis* arrangement (see Fig. 1) and the distance between the terminal groups for the former is considerably shorter than that for the latter (X-ray diffraction analysis), the PCA reaction rate of the latter with structure **B** is 3.5 times higher (see Fig. 2). Thus, the rate-determining step of photocycloaddition of compound **1a** should be the conformational transition from structure **A** to more reactive structure **B**. An indirect confirmation can be the mutual orientation of the β-protons of the four-membered cycle and the bridging oxygen atoms in the molecule of crown ether **2a** (oriented in the same direction) and the *s-cis* form of the chalcone groups at the moment of cyclization corresponding to structure **B**, which can be observed in the geometry of this molecule (see Fig. 3).

In turn, the low PCA rate in the case of chalcone-podand **1C** compared to **1b** (see Fig. 2) is related, most likely, to considerable conformational changes in the polyether chain during excimer formation.

The analysis of isolated photoadducts **2—5** (see Figs 3—6) by X-ray diffraction and ^{1}H and ^{13}C NMR spectroscopy revealed some regularities in the change in the geometric parameters of molecules of the homologs listed.

First, there is a certain dependence of the stereoisomerism type on the degree of folding of the cyclobutane ring of the photoadducts. The least angular strain[26] of the four-membered cycle is observed for *syn*-"head-to-tail" diastereomer **5c** (see Fig. 6). The "folding angle" φ between two root-mean-square planes passing through the C(8)C(9)C(29) and C(8)C(28)C(29) atoms is 2.3°, and the four-membered cycle is almost planar. For *anti*-"head-to-head" stereoisomers **2a** and **2b**, the angle φ is 15.8° (C(7)C(5)C(3)/C(3)C(8)C(7)) and 16.4° (C(8)C(9)C(34)/C(8)C(17)C(34)), respectively (see Fig. 3). The further increase in the folding angle is observed on going to the molecular structures of *syn*-"head-to-head" isomers **4b,c** with the angle φ equal to 25.3° (C(9)C(26)C(27)/C(9)C(8)C(27)) and 18.4° (C(28)C(9)C(8)/C(28)C(29)-C(8)), respectively (Fig. 5). The maximum deviations from the planar geometry of the cyclobutane fragment

Table 4. Bond lengths (*d*) and bond angles (ω) of the cyclobutane fragments in the crown ethers

Bond	*d*/Å	Bond angle	ω/deg
	rtct-**2a**		
C(5)—C(7)	1.549(2)	C(3)—C(5)—C(7)	89.4(9)
C(7)—C(8)	1.546(2)	C(5)—C(7)—C(8)	90.0(8)
C(8)—C(3)	1.563(2)	C(7)—C(8)—C(3)	89.9(9)
C(3)—C(5)	1.574(2)	C(8)—C(3)—C(5)	88.5(8)
	rtct-**2b**		
C(9)—C(8)	1.528(3)	C(9)—C(8)—C(17)	90.2(16)
C(8)—C(17)	1.565(3)	C(8)—C(17)—C(34)	88.9(14)
C(34)—C(17)	1.565(3)	C(17)—C(34)—C(9)	88.6(15)
C(9)—C(34)	1.573(3)	C(34)—C(9)—C(8)	90.0(14)
	rtcc-**3b**		
C(8)—C(9)	1.586(2)	C(8)—C(9)—C(26)	86.7(13)
C(9)—C(26)	1.564(2)	C(9)—C(26)—C(27)	90.6(13)
C(26)—C(27)	1.538(2)	C(26)—C(27)—C(8)	88.8(12)
C(8)—C(27)	1.553(2)	C(27)—C(8)—C(9)	89.2(12)
	rtcc-**3c**		
C(8)—C(9)	1.542(2)	C(8)—C(9)—C(28)	90.6(11)
C(9)—C(28)	1.561(2)	C(9)—C(28)—C(29)	85.3(11)
C(28)—C(29)	1.582(2)	C(28)—C(29)—C(8)	89.6(11)
C(8)—C(29)	1.546(1)	C(29)—C(8)—C(9)	87.2(11)
	rctt-**4b**		
C(8)—C(9)	1.539(2)	C(8)—C(9)—C(26)	88.3(14)
C(9)—C(26)	1.579(2)	C(9)—C(26)—C(27)	87.9(13)
C(26)—C(27)	1.568(2)	C(26)—C(27)—C(8)	88.3(13)
C(27)—C(8)	1.551(2)	C(27)—C(8)—C(9)	89.9(13)
	rctt-**4c**		
C(8)—C(9)	1.546(3)	C(8)—C(9)—C(28)	88.8(17)
C(9)—C(28)	1.575(3)	C(9)—C(28)—C(29)	88.7(17)
C(28)—C(29)	1.560(3)	C(28)—C(29)—C(8)	89.3(17)
C(8)—C(29)	1.547(3)	C(29)—C(8)—C(9)	90.3(18)
	5c *syn*-"head-to-tail"		
C(8)—C(9)	1.575(2)	C(8)—C(9)—C(28)	89.3(10)
C(9)—C(29)	1.545(2)	C(9)—C(29)—C(28)	90.7(10)
C(28)—C(29)	1.582(2)	C(8)—C(28)—C(29)	89.0(10)
C(8)—C(28)	1.544(2)	C(9)—C(8)—C(28)	91.0(9)

are characteristic of *rtcc*-isomers **3b** and **3c**; the angle φ is 23.3° (C(9)C(8)C(27)/C(9)C(26)C(27)) and 29.1° (C(28)C(29)C(8)/C(28)C(9)C(8)), respectively (see Fig. 4). The change in the degree of folding of the cyclobutane fragment in the series of homologs **5—2—4—3** agrees with an increase in the dispersion of the bond angle values of the four-membered cycle from the optimum value. The maximum scatter of the values from 90.6° (C(8)C(9)C(28)) to 85.3° (C(9)C(28)C(29)) was observed for stereoisomer **3c** (Table 4). It can be assumed that the folding angle value of the four-membered cycle depends primarily on the rotation of the phenyl substituents, whose orientation is controlled, in turn, by the polyether chain length. In the general case, the elongation of the oxyethylene fragment in the studied crown ethers, except for compounds **4b,c**, increases the angle φ and also decreases the torsional strain of the cycle but, probably, increases its stabilization.[26]

Differences in symmetry of photocycloaddition products **2—5** are also manifested in the NMR spectra. In stereoisomers *rtcc*-**2** and *rctt*-**4** assigned to the point symmetry groups C_2 and C_S, respectively, the cyclic protons form the AA′BB′ spin system. In the ^{13}C NMR spectra, the signals for the carbon atoms are equivalent in pairs (Fig. 7, see Table 3), whereas in isomers *rtcc*-**3** and *rctt*-**5** (point symmetry C_1) all protons and carbon atoms are chemically nonequivalent (see Fig. 7, Table 3).

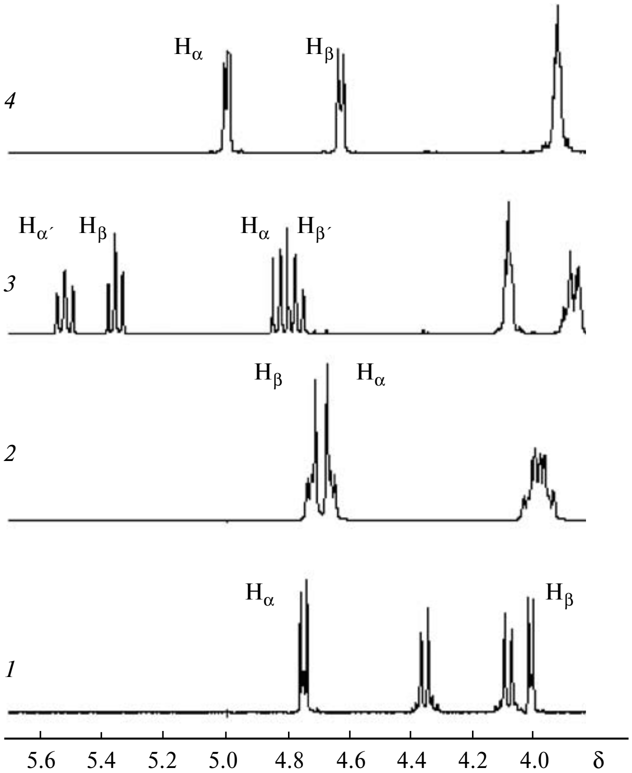

Fig. 7. Fragments of the ^{1}H NMR spectra (400 MHz, DMSO-d$_6$) for the cyclobutane protons in compounds **2a** (*1*), **2b** (*2*), **3b** (*3*), and **4b** (*4*).

In symmetric isomers **2** and **4**, the H(β,β′) protons are identified by the cross-peaks with the C(2) and C(6) carbon atoms in the HMBC spectrum, and the H(α,α′) protons are identified by the cross-peaks with the *ipso*-C atom of the phenyl substituent (the enumeration of atoms is given in Experimental).

The α,β-protons in nonsymmetric isomers **3b,c** were assigned similarly, and the differentiation between the α- and α′-protons is based on the comparison of the results of 2D NOESY experiments and X-ray diffraction data for compound **3c**. The NOESY spectrum exhibits cross-peaks between the $H_α$ and $H_β$ protons, and the latter, in turn, gives the cross-peak with the $H_{β′}$ proton. However, these three protons have no cross-peaks with the most low-field proton of the cyclic $H_{α′}$ protons ($δ_H$ 5.5), indicating its opposite orientation in the cycle. At the same time, rather intense cross-peaks between the $H_{α′}$ proton and the H(6), H(6′) protons are observed, which is consistent with the presence of the shortened contact between the corresponding protons in crystal, namely, r($H_{α′}$—H(6)) = 2.22 Å, r($H_{α′}$—H(6′)) = 2.30 Å. In addition, the NOESY spectrum exhibits the cross-peaks between the α,α′-protons and *ortho*-protons of the benzoyl substituents, *i.e.*, between the pairs ($H_α$—H(9)), ($H_{α′}$—H(9′)), which made it possible to identify the signals of the aromatic protons and then the carbon atoms by the 2D HSQC and HMBC spectra.

Thus, it was experimentally found that the presence of alkali metal cations, which can provide an additional intramolecular approach of the activated CH=CH bonds of the chalcone fragments due to complex formation, in solutions of chalcone-podands **1a—c** shifts the equilibrium to the concerted PCA reaction with the predominant formation of diastereomers **2a,b** and **4c**, respectively.

At the same time, the stereoselectivity of the PCA reaction depends, to a considerable extent, on the length of the oxyethylene fragment of the initial chalcone-podands. The shortest polyether chain in chalcone-podand **1a** (n = 0) favors the formation of *rtct*-isomer **2a**. In the case of compound **1b** (n = 1), *rtct*-**2b** and *rctt*-**4b** are formed equiprobably, whereas the chalcone-podand with the longest oxyethylene fragment (**1c**, n = 2) is dimerized predominantly to form *rctt*-**4c**. In turn, along with the polyether chain length, the stereoorientation of the terminal groups in compounds **1a—c** (the presence of the more reactive *trans-s-cis* conformation of the propenone fragment corresponding to structure **B**) can substantially affect the PCA rate.

Experimental

IR spectra were recorded on a Spectrum One FTIR spectrometer (Perkin—Elmer) using a diffuse reflectance sampling accessory (DRA). Electronic absorption spectra of the studied solutions were obtained on a UV-2401 PC spectrometer (Shimadzu) in quartz cells 1 cm thick. ^{1}H and ^{13}C NMR spectra were measured on a Bruker DRX-400 instrument with working frequencies of 400 and 100 MHz in a DMSO-d$_6$ solution using SiMe$_4$ and DMSO-d$_6$ (δ_C 39.5) as internal standards, respectively. The complete assignment of the ^{1}H and ^{13}C signals in the NMR spectra was performed by 2D COSY, NOESY, HSQC, and HMBC experiments. Mass spectra (EI) were recorded on a Varian MAT 311-A instrument. The energy of ionizing electrons was 70 eV, and the accelerating voltage was 3 eV. The melting points were determined on a Boetius microheating stage. Thin layer chromatography was carried out on Silufol-254 plates using an ethyl acetate—benzene (1 : 1) mixture as eluent and iodine vapor for detection.

Chalcone-podands **1a—c** were synthesized according to an earlier described procedure.[27]

1,2-Bis[2-(3-phenyl-3-oxoprop-1-en-1-yl)phenoxy)]ethane (1a). The yield was 87%, m.p. 142—144 °C. Calculated (%): C, 81.01; H, 5.48. $C_{32}H_{26}O_4$. Found (%): C, 81.09; H, 5.51. UV (DMF), λ/nm: 297 (logε 4.58), 344 (logε 3.11). ^{1}H NMR, δ: 4.63 (s, 4 H, O—C$\underline{\text{H}}_2$); 7.12 (ddd, 2 H, H(5), *J* = 7.7, 7.5 Hz, 1.0); 7.16 (dd, 4 H, H(3´), *J* = 8.3, 7.4 Hz); 7.30 (dd, 2 H, H(3), *J* = 8.4, 1.0 Hz); 7.47 (tt, 2 H, H(4´), *J* = 7.4, 1.3 Hz); 7.53 (ddd, 2 H, H(4), *J* = 8.4, 7.5, 1.7 Hz); 7.81 (dd, 4 H, H(2´), *J* = 8.3, 1.3 Hz); 7.83 (d, 2 H, H(6), *J* = 7.7 Hz); 7.86 (d, 2 H, H$_\beta$, *J* = 15.9 Hz); 8.02 (d, 2 H, H$_\alpha$, *J* = 15.9 Hz). ^{13}C NMR, δ: 67.00 (O—CH$_2$); 112.57 (C(3)); 121.12 (C(5)); 122.65 (C$_\alpha$); 123.07 (C(1)); 127.91 (C(2´)); 128.36 (C(3´)); 131.50 (C(6)); 132.14 (C(4)); 132.66 (C(4´)); 137.51 (C(1´)); 139.81 (C$_\beta$); 157.99 (C(2)); 189.09 (C=O). IR, ν/cm^{-1}: 693, 732, 749, 786 (arom.); 846, 870, 895, 944, 1001, 1018; 1059 (ν$_s$, C$_{\text{arom}}$—O—C$_{\text{Alk}}$); 1126, 1164, 1180 (ν$_{as}$, ν$_s$, C$_{\text{Alk}}$—O); 1203, 1239 (ν$_{as}$, C$_{\text{arom}}$—O—C$_{\text{Alk}}$); 1274, 1338, 1447, 1491; 1567, 1604 (δ, C=C); 1656 (δ, C=O); 2877, 2923, 2946 (δ, C$_{\text{Alk}}$—H); 3060, 3071 (δ, C$_{\text{arom}}$—H).

1,5-Bis[2-(3-phenyl-3-oxoprop-1-en-1-yl)phenoxy]-3-oxapentane (1b). The yield was 80%, m.p. 109—110 °C. Calculated (%): C, 78.76; H, 5.79. $C_{34}H_{30}O_5$. Found (%): C, 78.67; H, 5.7. UV (DMF), λ/nm: 297 (logε 4.47), 344 (logε 2.97). ^{1}H NMR, δ: 3.98 (m, 4 H, O—C$\underline{\text{H}}_2$); 4.26 (m, 4 H, Ar—O—C$\underline{\text{H}}_2$); 7.03 (dd, 2 H, H(5), *J* = 7.6, 7.3 Hz); 7.10 (d, 2 H, H(3), *J* = 8.4 Hz); 7.40 (ddd, 2 H, H(4), *J* = 8.4, 7.3, 1.6 Hz); 7.54 (m, 4 H, H(3´)); 7.63 (t, 2 H, H(4´), *J* = 7.3 Hz); 7.90 (dd, 2 H, H(6), *J* = 7.6, 1.6 Hz); 7.96 (d, 2 H, H$_\alpha$, *J* = 15.8 Hz); 8.02 (d, 2 H, H$_\beta$, *J* = 15.8 Hz); 8.09 (m, 4 H, H(2´)). ^{13}C NMR, δ: 67.77 (Ar—O—CH$_2$); 69.04 (O—CH$_2$); 112.88 (C(3)); 120.89 (C(5)); 122.33 (C$_\alpha$); 123.17 (C(1)); 128.27 (C(2´)); 128.67 (C(3´)); 129.58 (C(6)); 132.08 (C(4)); 132.86 (C(4´)); 137.77 (C(1´)); 139.15 (C$_\beta$); 157.67 (C(2)); 189.44 (C=O). IR, ν/cm^{-1}: 690, 730, 748, 784 (arom.); 817, 868, 967, 986, 1018; 1035, 1054 (ν$_s$, C$_{\text{arom}}$—O—C$_{\text{Alk}}$); 1117 (ν$_{as}$, ν$_s$, C$_{\text{Alk}}$—O—C$_{\text{Alk}}$); 1213, 1246 (ν$_s$, C$_{\text{arom}}$—O—C$_{\text{Alk}}$); 1275, 1328, 1447, 1491; 1567, 1598 (δ, C=C); 1650 (δ, C=O); 2827, 2881, 2945 (δ, C$_{\text{Alk}}$—H); 3001, 3058 (δ, C$_{\text{arom}}$—H).

1,8-Bis[2-(3-phenyl-3-oxoprop-1-en-1-yl)phenoxy)]-3,6-dioxaoctane (1c). The yield was 72%, oil. Calculated (%): C, 76.87; H, 6.05. $C_{36}H_{34}O_6$. Found (%): C, 76.54; H, 6.25. UV (DMF), λ/nm: 297 (logε 4.32), 344 (logε 2.22). ^{1}H NMR, δ: 3.68 (m, 4 H, O—C$\underline{\text{H}}_2$); 3.84 (m, 4 H, Ar—O—CH$_2$—C$\underline{\text{H}}_2$); 4.19 (m, 4 H, Ar—O—C$\underline{\text{H}}_2$—CH$_2$); 7.02 (dd, 2 H, H(5), *J* = 7.6, 7.3 Hz); 7.07 (d, 2 H, H(3), *J* = 8.4 Hz); 7.39 (ddd, 2 H, H(4), *J* = 8.4, 7.3, 1.6 Hz); 7.55 (m, 4 H, H(3´)); 7.63 (t, 2 H, H(4´), *J* = 7.3 Hz); 7.89 (dd, 2 H, H(6), *J* = 7.6, 1.6 Hz); 7.97 (d, 2 H, H$_\alpha$, *J* = 15.8 Hz); 8.00 (d, 2 H, H$_\beta$, *J* = 15.8 Hz); 8.09 (m, 4 H, H(2´)). ^{13}C NMR, δ: 67.68 (Ar—O—$\underline{\text{C}}$H$_2$—CH$_2$); 68.89 (Ar—O—CH$_2$—$\underline{\text{C}}$H$_2$); 69.94 (O—CH$_2$); 112.72 (C(3)); 120.81 (C(5)); 122.27 (C$_\alpha$); 123.07 (C(1)); 128.30 (C(2´)); 128.72 (C(3´)); 129.74 (C(6)); 132.09 (C(4)); 132.93 (C(4´)); 137.75 (C(1´)); 139.24 (C$_\beta$); 157.74 (C(2)); 189.40 (C=O). IR, ν/cm^{-1}: 665; 694, 734, 752 (arom.); 871, 935, 989, 1017; 1052, 1082 (ν$_s$, C$_{\text{arom}}$—O—C$_{\text{Alk}}$); 1117, 1125, 1163, 1180 (ν$_{as}$, ν$_s$, C$_{\text{Alk}}$—O—C$_{\text{Alk}}$); 1213, 1247 (ν$_{as}$, C$_{\text{arom}}$—O—C$_{\text{Alk}}$); 1275, 1333, 1448, 1489; 1571, 1598 (δ, C=C); 1659 (δ, C=O); 2874, 2945 (δ, C$_{\text{Alk}}$—H); 3063 (δ, C$_{\text{arom}}$—H).

Synthesis of cyclobutane-containing crown ethers. *A* (spectrophotometric studies). Solutions of initial chalcone-podands **1a—c** ($c = 5 \cdot 10^{-5}$ mol L^{-1}) in DMF in the absence and in the presence of an equimolar amount of KSCN (KClO$_4$, LiClO$_4$, CsClO$_4$) ($c = 5 \cdot 10^{-5}$ mol L^{-1}) in thin-walled glass vessels were irradiated with the nonfiltered light from the incandescent lamp (150 W) at a distance of 30 cm. The reaction course was monitored at certain time intervals by spectrophotometry (see Fig. 2).

B. Solutions of compounds **1a—c** (~0.01 g, 0.02 mmol) in the absence and in the presence of 0.02 mmole of KSCN (KClO$_4$) in DMF or MeCN (10 mL) in thin-walled glass vessels were irradiated with the nonfiltered light from the incandescent lamp (power 150 W) at a distance of 30 cm for 2—3 weeks. The duration of the PCA process was monitored by IR spectroscopy. After the completion of the reaction, the solvent was evaporated, and the ratio of photoadducts in the reaction mixtures was estimated by the comparison of integral intensities[28] of the signals for the α,β-protons of the *E*,*Z*-isomers and cyclobutane protons in the ^{1}H NMR spectra.

C. Solutions of compounds **1a—c** (~0.1 g, 0.2 mmol) in the absence and in the presence of 0.2, 0.6, and 1.2 mmole of KSCN (KClO$_4$) in 25 mL of DMF or MeCN in quartz vessels on cooling (16—18 °C) were irradiated for 24—32 h with the light from the mercury lamp (power 500 W) using light filters from the standard set of colored optical glasses in short-wavelength regions of 258—400 nm (transmission λ$_{\text{max}}$ was 366 nm) and 364—456 nm (transmission λ$_{\text{max}}$ was 405 nm) at a distance of 30 cm. The duration of the PCA process was monitored by IR spectroscopy. After the completion of the process, the solvent was evaporated, and the ratio of photoadducts in the reaction mixtures was estimated by the comparison of integral intensities of the signals for the α,β-protons of the *E*,*Z*-isomers and cyclobutane protons in the ^{1}H NMR spectra (see Table 2). The PCA products were separated by column chromatography (SiO$_2$) using benzene—ethyl acetate (1 : 1 or 5 : 1) and ethyl acetate—acetonitrile (25 : 1) mixtures as eluents.

(12*c*,13*t*,14*r*,15*t*)-13,14-Dibenzoyl-2,5-dioxatetracyclo[14.4.0.0^{6,11}.0^{12,15}]eucosa-1(16),6,8,10,17,19-hexaene (*rtct*-2a), m.p. 157—158 °C. Calculated (%): C, 81.01; H, 5.48. $C_{32}H_{26}O_4$. Found (%): C, 80.98; H, 5.49. ^{1}H NMR, δ: 4.01 (m, 2 H, H$_\beta$, H$_{\beta'}$); 4.08, 4.35 (both m, 2 H each, ArOC$\underline{\text{H}}_2$); 4.75 (m, 2 H, H$_\alpha$, H$_{\alpha'}$); 7.08—7.12 (m, 4 H, H(3), H(3´), H(5), H(5´)); 7.25 (td, 2 H, H(4), H(4´), *J* = 7.6, 1.6 Hz); 7.39 (dd, 4 H, H(10), H(10´), *J* = 8.2, 7.5 Hz); 7.43 (dd, 2 H, H(6), H(6´), *J* = 7.6, 1.6 Hz); 7.56 (tt, 2 H, H(11), H(11´), *J* = 7.5, 1.2 Hz); 7.83 (dd, 4 H, H(9), H(9´), *J* = 8.2, 1.2 Hz). ^{13}C NMR, δ: 41.85 (C$_\beta$, C$_{\beta'}$); 45.44 (C$_\alpha$, C$_{\alpha'}$); 70.57 (OCH$_2$); 118.68 (C(3),

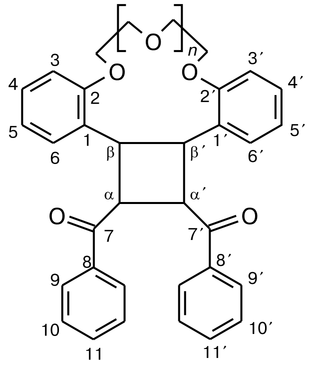

C(3´)); 122.99 (C(5), C(5´)); 127.12 (C(6), C(6´)); 127.82 (C(4), C(4´)); 128.33 (C(9), C(9´)); 128.67 (C(10), C(10´)); 133.62 (C(11), C(11´)); 134.12 (C(1), C(1´)); 134.91 (C(8), C(8´)); 157.20 (C(2), C(2´)); 198.81 (C(7), C(7´)). MS, *m/z* (I/I_{max} (%)): 474 $[M]^+$ (6), 456 (2), 369 (30), 223 (9), 222 (17), 207 (56), 178 (4), 165 (4), 145 (3), 131 (10), 105 (100), 77 (54), 55 (2). IR, ν/cm^{-1}: 617, 657, 669; 704, 761 (arom.); 854, 904, 956, 937, 988, 1001; 1058, 1089 (ν_s, C_{arom}—O—C_{Alk}); 1157, 1187 (ν_s, ν_{as}, C_{Alk}—O—C_{Alk}); 1216, 1245 (ν_{as}, C_{arom}—O—C_{Alk}); 1290, 1330, 1385, 1446, 1491; 1579, 1593 (δ, C=C); 1671 (δ, C=O); 2865, 2914, 2946 (δ, C_{Alk}—H); 3061 (δ, C_{arom}—H).

(15*c*,16*t*,17*r*,18*t*)-16,17-Dibenzoyl-2,5,8-trioxatetracyclo-[17.4.0.0^{9,14}.0^{15,18}]tricosa-1(19),9,11,13,20,22-hexaene (*rtct*-2b), m.p. 221—223 °C. Calculated (%): C, 78.76; H, 5.79. $C_{34}H_{30}O_5$. Found (%): C, 78.79; H, 5.74. ^{1}H NMR, δ: 3.55—3.60, 3.74—3.81 (both m, 2 H each, O—C$\underline{H}_2$); 3.93—4.05 (m, 4 H, ArOC$\underline{H}_2$); 4.65 (m, 2 H, H_α, $H_{\alpha'}$); 4.72 (m, 2 H, H_β, $H_{\beta'}$); 6.87—6.95 (m, 4 H, H(3), H(3´), H(5), H(5´)); 7.18 (td, 2 H, H(4), H(4´), *J* = 7.7, 1.5 Hz); 7.33—7.37 (m, 6 H, H(10), H(10´), H(6), H(6´)); 7.51 (tt, 2 H, H(11), H(11´), *J* = 7.3, 1.0 Hz); 7.68 (dd, 4 H, H(9), H(9´), *J* = 8.3, 1.0 Hz). ^{13}C NMR, δ: 41.83 (C_β, $C_{\beta'}$); 46.59 (C_α, $C_{\alpha'}$); 69.03 (O—CH$_2$); 70.23 (ArOCH$_2$); 115.54 (C(3), C(3´)); 121.40 (C(5), C(5´)); 128.05 (C(9), C(9´)); 128.28 (C(4), C(4´)); 128.39 (C(10), C(10´)); 129.34 (C(6), C(6´)); 129.88 (C(1), C(1´)); 133.10 (C(11), C(11´)); 136.14 (C(8), C(8´)); 158.40 (C(2), C(2´)); 198.86 (C(7), C(7´)). MS, *m/z* (I/I_{max} (%)): 518 $[M]^+$ (3), 500 (3), 413 (28), 398 (2), 282 (5), 236 (4), 228 (8), 207 (39), 178 (3), 165 (5), 145 (2), 131 (12), 105 (100), 77 (37), 55 (2). IR, ν/cm^{-1}: 660; 696, 761, 779 (arom.); 801, 903, 924, 982, 1019; 1048 (ν_s, C_{arom}—O—C_{Alk}); 1127, 1145, 1182 (ν_s, ν_{as}, C_{Alk}—O—C_{Alk}); 1209, 1223, 1244 (ν_{as}, C_{arom}—O—C_{Alk}); 1271, 1295, 1318, 1451, 1489; 1580, 1597 (δ, C=C); 1669, 1680 (δ, C=O); 2889, 2919, 2945 (δ, C_{Alk}—H); 3013, 3058 (δ, C_{arom}—H).

(15*c*,16*t*,17*r*,18*c*)-16,17-Dibenzoyl-2,5,8-trioxatetracyclo-[17.4.0.0^{9,14}.0^{15,18}]tricosa-1(19),9,11,13,20,22-hexane (*rtcc*-3b), m.p. 219—221 °C. Calculated (%): C, 78.76; H, 5.79. $C_{34}H_{30}O_5$. Found (%): C, 78.74; H, 5.78. ^{1}H NMR, δ: 3.40—3.52 (m, 2 H, OC$\underline{H}_2$); 3.60 (dt, 1 H, OC$\underline{H}_2$, *J* = 11.3, 2.4 Hz); 3.75 (m, 1 H, ArOC$\underline{H}_2$); 3.84—3.92 (m, 2 H, ArOC$\underline{H}_2$ and OC$\underline{H}_2$); 4.04—4.13 (m, 2 H, ArOC$\underline{H}_2$); 4.74—4.86 (m, 2 H, $H_{\beta'}$, H_α); 5.35 (dd, 1 H, H_β, *J* = 10.3, 9.6 Hz); 5.52 (dd, $H_{\alpha'}$, *J* = 10.3, 10.2 Hz); 6.42 (ddd, 1 H, H(5), *J* = 7.7, 7.3, 1.1 Hz); 6.60 (dd, 1 H, H(3), *J* = 8.3, 1.1 Hz); 6.66 (dd, 1 H, H(3´), *J* = 7.9, 0.9 Hz); 6.75 (ddd, 1 H, H(4), *J* = 8.3, 7.3, 1.6 Hz); 6.80 (ddd, 1 H, H(5´), *J* = 7.6, 7.4, 0.9 Hz); 6.85 (dd, 1 H, H(6), *J* = 7.7, 1.6 Hz); 7.02 (ddd, 1 H, H(4´), *J* = 7.9, 7.6, 1.6 Hz); 7.27—7.33 (m, 3 H, H(10), H(6´)); 7.45 (tt, 1 H, H(11), *J* = 7.4, 1.3 Hz); 7.52—7.57 (m, 2 H, H(10´)); 7.64 (tt, 1 H, H(11´), *J* = 7.4, 1.4 Hz); 7.70—7.73 (m, 2 H, H(9)); 8.23—8.26 (m, 2 H, H(9´)). ^{13}C NMR, δ: 37.88 ($C_{\beta'}$); 38.64 (C_β); 41.64 ($H_{\alpha'}$); 48.22 (H_α); 63.93 ($\underline{C}$H$_2$OAr´); 65.76 (O—CH$_2$); 67.20 (O—CH$_2$); 67.81 ($\underline{C}$H$_2$OAr); 110.37 (C(3)); 114.23 (C(3´)); 119.31 (C(5)); 119.66 (C(5´)); 126.71 and 126.76 (C(4) and C(1´)); 127.29 and 127.32 (C(4´) and C(6´)); 127.42 (C(1)); 128.06 and 128.09 (C(9) and C(10)); 128.69 and 128.71 (C(9´) and C(10´)); 129.18 (C(6)); 132.96 (C(11)); 133.47 (C(11´)); 135.19 (C(8)); 135.88 (C(8´)); 155.66 (C(2)); 155.70 (C(2´)); 197.54 (C(7)); 199.97 (C(7´)). IR, ν/cm^{-1}: 558, 606, 623; 689, 701, 710, 745, 754, 788 (arom.); 827, 843, 900, 913, 920, 935, 984, 1010, 1023; 1039, 1064 (ν_s, C_{arom}—O—C_{Alk}); 1102, 1127, 1142, 1180 (ν_s, ν_{as}, C_{Alk}—O—C_{Alk}); 1212, 1224, 1249 (ν_{as}, C_{arom}—O—C_{Alk}); 1324, 1450, 1489; 1581, 1596 (δ, C=C); 1669 (δ, C=O); 2854, 2896, 2948, 2984 (δ, C_{Alk}—H); 3032, 3050 (δ, C_{arom}—H).

(18*c*,19*t*,20*r*,21*c*)-19,20-Dibenzoyl-2,5,8,11-tetraoxatetracyclo[20.4.0.0^{12,17}.0^{18,21}]hexacosa-1(22),12,14,16,23,25-hexaene (*rtcc*-3c), m.p. 213—215 °C. Calculated (%): C, 76.87; H, 6.05. $C_{36}H_{34}O_6$. Found (%): C, 76.88; H, 6.07. ^{1}H NMR, δ: 3.15 (m, 1 H, OC$\underline{H}_2$); 3.53—3.62 (m, 2 H, ArOC$\underline{H}_2$); 3.70—3.97 (m, 9 H, OC$\underline{H}_2$ and ArOC$\underline{H}_2$); 4.78 (dd, 1 H, $H_{\beta'}$, *J* = 10.5, 10.2 Hz); 4.86 (dd, 1 H, H_α, *J* = 10.1, 9.1 Hz); 5.29 (dd, 1 H, H_β, *J* = 10.2, 10.1 Hz); 5.49 (dd, 1 H, $H_{\alpha'}$, *J* = 10.5, 9.1 Hz); 6.33 (dd, 1 H, H(3), *J* = 8.1, 1.1 Hz); 6.40 (td, 1 H, H(5), *J* = 7.6, 1.1 Hz); 6.64 (dd, 1 H, H(3´), *J* = 8.0, 1.0 Hz); 6.75 (ddd, 1 H, H(4), *J* = 8.1, 7.6, 1.7 Hz); 6.80 (dd, 1 H, H(6), *J* = 7.6, 1.7 Hz); 6.84 (ddd, 1 H, H(5´), *J* = 7.6, 7.5, 1.0 Hz); 7.05 (ddd, 1 H, H(4´), *J* = 8.0, 7.6, 1.7 Hz); 7.24—7.31 (m, 3 H, H(10), H(6´)); 7.44 (tt, 1 H, H(11), *J* = 7.4, 1.2 Hz); 7.55—7.60 (m, 2 H, H(10´)); 7.64—7.69 (m, 3 H, H(11´) and H(9)); 8.30—8.33 (m, 2 H, H(9´)). ^{13}C NMR, δ: 37.47 ($C_{\beta'}$); 38.26 (C_β); 41.83 ($C_{\alpha'}$); 49.04 (C_α); 66.03, 66.59, 68.26, 68.91, 69.30, 72.20 (5 OCH$_2$); 109.42 (C(3)); 110.35 (C(3´)); 118.42 (C(5)); 119.85 (C(5´)); 125.16 (C(1)); 126.84 (C(6´) and C(1´)); 126.96 (C(4)); 127.42 (C(4´)); 127.76 (C(10)); 127.98 (C(9)); 128.74 and 128.79 (C(10´), C(9´), C(6)); 132.74 (C(11)); 133.53 (C(11´)); 135.03 (C(8)); 135.93 (C(8´)); 155.78 (C(2)); 156.19 (C(2´)); 197.32 (C(7)); 200.01 (C(7´)). IR, ν/cm^{-1}: 478, 504, 637, 659; 691, 712, 752, 791 (arom.); 835, 847, 924, 953; 1064, 1074 (ν_s, C_{arom}—O—C_{Alk}); 1106, 1117, 1142 (ν_s, ν_{as}, C_{Alk}—O—C_{Alk}); 1229, 1253 (ν_{as}, C_{arom}—O—C_{Alk}); 1304, 1316, 1338, 1407, 1447, 1492; 1581, 1597 (δ, C=C); 1662, 1679 (δ, C=O); 2863, 2925 (δ, C_{Alk}—H); 3029, 3058 (δ, C_{arom}—H).

(15*t*,16*c*,17*r*,18*t*)-16,17-Dibenzoyl-2,5,8-trioxatetracyclo-[17.4.0.0^{9,14}.0^{15,18}]tricosa-1(19),9,11,13,20,22-hexaene (*rctt*-4b), m.p. 180—182 °C. Calculated (%): C, 78.76; H, 5.79. $C_{34}H_{30}O_5$. Found (%): C, 78.77; H, 5.76. ^{1}H NMR, δ: 3.58 (m, 4 H, OC$\underline{H}_2$); 3.93 (m, 4 H, ArOC$\underline{H}_2$); 4.63 (m, 2 H, H_β, $H_{\beta'}$); 5.00 (m, 2 H, H_α, $H_{\alpha'}$); 6.74—6.78 (m, 4 H, H(3), H(3´), H(5), H(5´)); 7.02 (td, 2 H, H(4), H(4´), *J* = 8.0, 1.6 Hz); 7.38—7.43 (m, 6 H, H(10), H(10´), H(6), H(6´)); 7.52 (tt, 2 H, H(11), H(11´), *J* = 7.4, 1.3 Hz); 7.81 (dd, 4 H, H(9), H(9´), *J* = 8.3, 1.3 Hz). ^{13}C NMR, δ: 37.74 (C_β, $C_{\beta'}$); 47.24 (C_α, $C_{\alpha'}$); 65.31 (ArO$\underline{C}$H$_2$); 66.21 (OCH$_2$); 111.60 (C(3), C(3´)); 119.71 (C(5), C(5´)); 127.16 (C(4), C(4´)); 127.80 (C(9), C(9´)); 128.08 (C(6), C(6´)); 128.12 (C(1), C(1´)); 128.59 (C(10), C(10´)); 132.92 (C(11), C(11´)); 135.53 (C(8), C(8´)); 155.40 (C(2), C(2´)); 198.53 (C(7), C(7´)). IR, ν/cm^{-1}: 479, 562, 603; 691, 714, 752, 775, 789 (arom.); 853, 914, 942, 1001; 1055, 1087 (ν_s,

C_{arom}—O—C_{Alk}); 1116, 1144, 1164, 1185 (ν_s, ν_{as}, C_{Alk}—O—C_{Alk}); 1224, 1243 (ν_{as}, C_{arom}—O—C_{Alk}); 1300, 1322, 1338, 1353, 1447, 1489; 1580, 1598 (δ, C=C); 1672, 1683 (δ, C=O); 2859, 2932, 2962 (δ, C_{Alk}—H); 3037, 3063 (δ, C_{arom}—H).

(18*t*,19*c*,20*r*,21*t*)-19,20-Dibenzoyl-2,5,8,11-tetraoxatetracyclo[20.4.0.0^{12,17}.0^{18,21}]hexacosa-1(22),12,14,16,23,25-hexaene (*rctt*-4c), m.p. 218—220 °C. Calculated (%): C, 76.87; H, 6.05. $C_{36}H_{34}O_6$. Found (%): C, 76.9; H, 6.12. ^{1}H NMR, δ: 3.19—3.27 (m, 2 H, O—C$\underline{H}_2$); 3.46 (m, 4 H, O—C$\underline{H}_2$); 3.66—3.75 (m, 4 H, O—C$\underline{H}_2$); 3.77—3.83 (m, 2 H, O—C$\underline{H}_2$); 4.60 (m, 2 H, H_β, $H_{\beta'}$); 4.93 (m, 2 H, H_α, $H_{\alpha'}$); 6.71—6.79 (m, 4 H, H(3), H(3´), H(5), H(5´)); 7.06 (td, 2 H, H(4), H(4´), *J* = 7.7, 1.7 Hz); 7.33 (dd, 2 H, H(6), H(6´), *J* = 7.6, 1.7 Hz); 7.42 (dd, 4 H, H(10), H(10´), *J* = 8.0, 7.5 Hz); 7.54 (tt, 2 H, H(11), H(11´), *J* = 7.5, 1.2 Hz); 7.81 (dd, 4 H, H(9), H(9´), *J* = 8.0, 1.2 Hz). ^{13}C NMR, δ: 34.75 (C_β, $C_{\beta'}$); 48.83 (C_α, $C_{\alpha'}$); 66.79 (ArO$\underline{C}H_2$); 68.41 (OCH_2); 70.64 (O—CH_2); 110.38 (C(3), C(3´)); 119.64 (C(5), C(5´)); 127.24 (C(4), C(4´)); 127.78 (C(6), C(6´)); 128.0 (C(9), C(9´)); 128.28 (C(1), C(1´)); 128.46 (C(10), C(10´)); 132.84 (C(11), C(11´)); 135.53 (C(8), C(8´)); 155.93 (C(2), C(2´)); 198.41 (C(7), C(7´)). MS, *m/z* (I/I_{max} (%)): 562 $[M]^+$ (2), 457 (19), 223 (4), 207 (31), 178 (2), 165 (5), 145 (2), 131 (7), 105 (100), 77 (32), 55 (2). IR, ν/cm^{-1}: 559, 609, 639; 693, 711, 748, 773, 788 (arom.); 853, 918, 951, 1003; 1060 (ν_s, C_{arom}—O—C_{Alk}); 1115, 1136, 1160 (ν_s, ν_{as}, C_{Alk}—O—C_{Alk}); 1225, 1252 (ν_{as}, C_{arom}—O—C_{Alk}); 1290, 1319, 1365, 1448, 1492; 1581, 1598 (δ, C=C); 1669, 1681 (δ, C=O); 2865, 2913 (δ, C_{Alk}—H); 3035, 3065 (δ, C_{arom}—H).

(1*t*,24*c*,25*r*,26*t*)-25,26-Dibenzoyl-8,11,14,17-tetraoxatetracyclo[22.1.1.0^{2,7}.0^{18,23}]hexacosa-2,4,6,18,20,22-hexaene (*rtcc*-5c), m.p. 219—221 °C. Calculated (%): C, 76.87; H, 6.05. $C_{36}H_{34}O_6$. Found (%): C, 76.84; H, 6.09. ^{1}H NMR, δ: 3.54 (m, 1 H, OC$\underline{H}_2$); 3.75—3.89 (m, 8 H, OC$\underline{H}_2$); 4.03, 4.11, 4.34 (all m, 1 H each, OC$\underline{H}_2$); 4.70 (ddd, 1 H, C$\underline{H}$, *J* = 12.0, 8.2, 0.8 Hz); 4.85 (ddd, 1 H, C$\underline{H}$, *J* = 12.0, 6.8, 0.8 Hz); 5.09 (ddd, 1 H, C$\underline{H}$, *J* = 11.8, 6.8, 0.8 Hz); 5.66 (ddd, 1 H, C$\underline{H}$, *J* = 11.8, 8.2, 0.8 Hz); 6.52—6.58 (m, 2 H, Ar); 6.63 (dd, 1 H, Ar, *J* = 8.1, 1.0 Hz); 6.79 (td, 1 H, Ar, *J* = 7.5, 1.1 Hz); 6.88—6.98 (m, 2 H, Ar); 7.04 (dd, 1 H, Ar, *J* = 7.5, 1.7 Hz); 7.19—7.24 (m, 2 H, Ar); 7.26—7.36 (m, 4 H, Ar); 7.42 (tt, 1 H, Ar, *J* = 7.3, 1.4 Hz); 7.64—7.70 (m, 4 H, Ar). IR, ν/cm^{-1}: 478, 498, 597, 612; 687, 697, 730, 756, 772 (arom.); 806, 850, 911, 926, 938; 1060 (ν_s, C_{arom}—O—C_{Alk}); 1116, 1138 (ν_s, ν_{as}, C_{Alk}—O—C_{Alk}); 1235, 1251 (ν_{as}, C_{arom}—O—C_{Alk}); 1278, 1296, 1320, 1367, 1448, 1493; 1584, 1598 (δ, C=C); 1668 (δ, C=O); 2874, 2923, 2964 (δ, C_{Alk}—H); 3038, 3061 (δ, C_{arom}—H).

X-ray diffraction study. Crystals of cyclobutane-containing crown ethers **2a,b** were prepared by the slow concentration of solutions in DMF, compounds **3b,c** were obtained in acetonitrile, compounds **4b,c** were obtained from *n*-butanol, and crystals of compound **5c** were prepared from benzene. Single crystals of compounds **2a**, **3b,c**, **4b,c**, and **5c** are racemates, whereas single crystals of earlier[27] described compound **2b** represent a conglomerate and are formed by molecules of the *R*,*R*,*S*,*S*- or *S*,*S*,*R*,*R*-enantiomer. X-ray diffraction analysis of the compounds was carried out on an Xcalibur 3 automated diffractometer with the CCD detector (MoKα radiation, λ = 0.71073 Å, graphite monochromator, *T* = 295 K). The structures were solved by a direct method and refined by least squares first in the isotropic and then in the anisotropic approximation by F^2 for all nonhydrogen atoms using the SHELXS-97 and SHELXL-97 programs.[28] Some hydrogen atoms were revealed in the difference synthesis and included into the refinement in the isotropic approximation, and some hydrogen atoms were placed in geometrically calculated positions and refined using the riding model.

Compound *rtct*-**2a** (solvate): $C_{32}H_{26}O_4 \cdot C_3H_7ON$, $M = 547.62$, the crystals are triclinic, space group *P*1, $a = 9.5686(4)$ Å, $b = 11.2901(4)$ Å, $c = 14.2661(5)$ Å, $\alpha = 82.179(3)°$, $\beta = 84.403(4)°$, $\gamma = 73.307(4)°$, $V = 1459.72(9)$ Å^3; $Z = 2$, $\mu = 0.083$ cm^{-1}; 13 505 measured reflections ($2.70 < \theta < 31.61°$), of them 7966 were independent reflections ($R_{int} = 0.0140$), number of reflections with $I > 2\sigma(I)$ 4768, $\rho = 1.246$ g cm^{-3}, *R* factors: $R_1 = 0.0782$, $wR_2 = 0.1370$ (for all reflections), $R_1 = 0.0461$, $wR_2 = 0.1267$ ($I > 2\sigma(I)$).

Compound *rtcc*-**3b**: $C_{34}H_{30}O_5$, $M = 518.58$, the crystals are monoclinic, space group *P*2(1)/*C*, $a = 19.361(4)$ Å, $b = 13.2285(18)$ Å, $c = 10.433(2)$ Å, $\beta = 91.980(17)°$, $V = 2670.5(9)$ Å^3; $Z = 4$, $\mu = 0.086$ cm^{-1}; 17 028 measured reflections ($2.61 < \theta < 26.38°$), of them 5332 were independent reflections ($R_{int} = 0.0542$), number of reflections with $I > 2\sigma(I)$ 2052, $\rho = 1.290$ g cm^{-3}, *R* factors: $R_1 = 0.1535$, $wR_2 = 0.0538$ (for all reflections), $R_1 = 0.0413$, $wR_2 = 0.0481$ ($I > 2\sigma(I)$).

Compound *rtcc*-**3c**: $C_{36}H_{34}O_6$, $M = 562.63$, the crystals are monoclinic, space group *P*2(1)/*C*, $a = 11.5545(6)$ Å, $b = 22.9959(12)$ Å, $c = 11.1039(7)$ Å, $\beta = 90.019(5)°$, $V = 2950.4(3)$ Å^3; $Z = 4$, $\mu = 0.085$ cm^{-1}; 25 755 measured reflections ($2.70 < \theta < 26.39°$), of them 5984 were independent reflections ($R_{int} = 0.0645$), number of reflections with $I > 2\sigma(I)$ 2341, $\rho = 1.267$ g cm^{-3}, *R* factors: $R_1 = 0.1392$, $wR_2 = 0.0457$ (for all reflections), $R_1 = 0.0429$, $wR_2 = 0.0422$ ($I > 2\sigma(I)$).

Compound *rctt*-**4b**: $C_{34}H_{30}O_5$, $M = 518.58$, the crystals are orthorhombic, space group *Pbca*, $a = 11.9378(11)$ Å, $b = 19.208(2)$ Å, $c = 23.338(2)$ Å, $\beta = 90°$, $V = 5351.4(9)$ Å^3; $Z = 8$, $\mu = 0.086$ cm^{-1}; 24 767 measured reflections ($2.66 < \theta < 26.39°$), of them 5399 were independent reflections ($R_{int} = 0.0840$), number of reflections with $I > 2\sigma(I)$ 2051, $\rho = 1.287$ g cm^{-3}, *R* factors: $R_1 = 0.1545$, $wR_2 = 0.0649$ (for all reflections), $R_1 = 0.0441$, $wR_2 = 0.0591$ ($I > 2\sigma(I)$).

Compound *rctt*-**4c**: $C_{36}H_{34}O_6$, $M = 562.63$, the crystals are orthorhombic, space group *Pccn*, $a = 14.4068(9)$ Å, $b = 34.171(4)$ Å, $c = 11.8808(14)$ Å, $\beta = 90°$, $V = 5848.9(11)$ Å^3; $Z = 8$, $\mu = 0.086$ cm^{-1}; 21 394 measured reflections ($2.83 < \theta < 26.38°$), of them 5847 were independent reflections ($R_{int} = 0.0973$), number of reflections with $I > 2\sigma(I)$ 2112, $\rho = 1.278$ g cm^{-3}, *R* factors: $R_1 = 0.1781$, $wR_2 = 0.0916$ (for all reflections), $R_1 = 0.0570$, $wR_2 = 0.0812$ ($I > 2\sigma(I)$).

Compound *rctt*-**5c** (solvate): $C_{36}H_{34}O_6 \cdot C_6H_6 \cdot H_2O$, $M = 658.76$, the crystals are triclinic, space group *P*1, $a = 9.0980(14)$ Å, $b = 13.682(3)$ Å, $c = 14.6328(13)$ Å, $\alpha = 84.709(14)°$, $\beta = 89.163(9)°$, $\gamma = 71.474(14)°$, $V = 1719.5(4)$ Å^3; $Z = 2$, $\mu = 0.086$ cm^{-1}; 17 477 measured reflections ($2.71 < \theta < 28.28°$), of them 8111 were independent reflections ($R_{int} = 0.0258$), number of reflections $I > 2\sigma(I)$ 3811, $\rho = 1.272$ g cm^{-3}, *R* factors: $R_1 = 0.1060$, $wR_2 = 0.0857$ (for all reflections), $R_1 = 0.0410$, $wR_2 = 0.0784$ ($I > 2\sigma(I)$).

This work was financially supported by the Russian Foundation for Basic Research (Project Nos 07-03-96111 and 07-03-96113) and the Presidium of the Russian Academy of Sciences (Project "Design of New Supramolecular Structures Containing Heterocyclic Fragments").

References

1. M. V. Alfimov, O. A. Fedorova, S. P. Gromov, *J. Photochem. Photobiol. A: Chem.*, 2003, **158**, 183.
2. J. Svoboda, B. König, *Chem. Rev.*, 2006, **106**, 5413.
3. J.-M. Lehn, *Supramolecular Chemistry. Concepts and Perspectives*, VCH, Weinheim, 1995, Ch. 8.
4. M. Nogradi, *Stereoselective Synthesis. A Practical Approach*, Weinheim (FRG): VCH Verlag mbh, 1995, Ch. 7, pp. 257—292.
5. G. Montaudo, S. Caccamese*, J. Org. Chem.*, 1973, **38**, 710.
6. E. Karpuk, D. Schollmeyer, H. Meier, *Eur. J. Org. Chem.*, 2007, 1983.
7. H. Hopf, H. Greiving, C. Beck, I. Dix, P. G. Jones, J.-P. Desvergne, H. Bouas-Laurent, *Eur. J. Org. Chem.*, 2005, 567.
8. H. Greiving, H. Hopf, C. Beck, P. G. Jones, P. Bubenitschek, J.-P. Desvergne, H. Bouas-Laurent, *Eur. J. Org. Chem.*, 2005, 558.
9. F. Cibin, N. Bello, G. Doddi, V. Fares, P. Mencarelli, *Tetrahedron*, 2003, **59**, 3455.
10. F. Cibin, N. Bello, G. Doddi, V. Fares, P. Mencarelli, E. Ullucci, *Tetrahedron*, 2003, **59**, 9971.
11. S. Akabori, T. Kumacai, Y. Habata, S. Sato, *Bull. Chem. Soc. Jpn.*, 1988, **61**, 2459.
12. S. Inokuma, T. Yamamoto, J. Nishimura, *Tetrahedron Lett.*, 1990, **31**, 97.
13. S. Inokuma, S. Sakai, R. Katon, J. Nishimura, *Bull. Chem. Soc. Jpn.*, 1994, **67**, 1462.
14. S. Inokuma, K. Kimura, T. Funaki, J. Nishimura, *J. Inclusion Phenomena Macrocyclic Chem.*, 2001, **39**, 35.
15. J. A. Ors, R. Srinivasan, *J. Am. Chem. Soc.*, 1978, **100**, 315.
16. K. Hiratani, S. Aiba, *Bull. Chem. Soc. Jpn.*, 1984, **57**, 2657.
17. I. G. Ovchinnikova, O. V. Fedorova, P. A. Slepukhin, I. A. Litvinov, G. L. Rusinov, *Kristallografiya*, 2009, **54**, No. 1, 32 [*Crystallogr. Repts* (*Engl. Transl.*), 2009, No. 1].
18. F. A. Carey, R. J. Sundberg, *Advanced Organic Chemistry. Part A; Structure and Mechanisms, 5. Photochemistry*, Springer, US, 2007, **12**, 1073.
19. S. A. Fleming, A. A. Parent, E. E. Parent, J. A. Pincock, L. Renault, *J. Org. Chem.*, 2007, **72**, 9464.
20. A. I. Vedernikov, S. P. Gromov, N. A. Lobova, L. G. Kuz´mina, Yu. A. Strelenko, J. A. K. Howard, M. V. Alfimov, *Izv. Akad. Nauk*, *Ser. Khim.*, 2005, **54**, 1896 [*Russ. Chem. Bull., Int. Ed.*, 2005, 1954].
21. F. M. Menger, J. H. Smith, *J. Am. Chem. Soc.*, 1969, 4211.
22. E. Weber, J. L. Toner, I. Goldberg, F. Vögtle, D. A. Laidler, J. F. Stoddart, R. A. Bartsch, C. L. Liotta, *Crown Ethers and Analogs*, John Wiley & Sons, Chichester, 1989, Ch. 2, pp. 3—15.
23. *Host Guest Complex Chemistry Macrocycles. Synthesis, Structures, Applications*, Eds F. Vögtle, E. Weber, Springer-Verlag, Berlin, 1985.
24. J. W. Steed, J. I. Atwood, *Supramolecular Chemistry*, John Wiley & Sons, Chichester, 2000, Ch. 3.9.
25. S. N. Gromov, A. N. Vedernikov, Yu. V. Fedorov, O. A. Fedorova, E. N. Andryukhina, N. E. Shepel´, Yu. A. Strelenko, D. Johnels, U. Edlund, J. Saltiel, M. V. Alfimov, *Izv. Akad. Nauk*, *Ser. Khim.*, 2005, 1524 [*Russ. Chem. Bull.*, *Int. Ed.*, 2005, **54**, 1569].
26. R. M. Moriarty, *Top. Stereochem.,* 1973, **8**, 271.
27. I. G. Ovchinnikova, O. V. Fedorova, P. A. Slepukhin, G. L. Rusinov, *Izv. Akad. Nauk*, *Ser. Khim.*, 2008, 204 [*Russ. Chem. Bull.*, *Int. Ed.*, 2008, **57**, 209].
28. G. M. Sheldrick, *Acta Crystallogr.*, *Sect. A*, 2008, **64**, 112.

Received March 25, 2009